

## Article

# Effects of Sequential Operation with Heat Treatment and Mechanical Milling on Work Hardening for Superalloy GH4169

Pingzhong Zhu <sup>1,2</sup>, Zhanqiang Liu <sup>1,2,\*</sup> , Xiaoping Ren <sup>1,2</sup>, Bing Wang <sup>1,2</sup> and Qinghua Song <sup>1,2</sup> 

<sup>1</sup> School of Mechanical Engineering, Shandong University, Jinan 250061, China; sdzhu pingzhong@mail.sdu.edu.cn (P.Z.); renxiaoping@sdu.edu.cn (X.R.); sduwangbing@sdu.edu.cn (B.W.); ssinghua@sdu.edu.cn (Q.S.)

<sup>2</sup> Key National Demonstration Center for Experimental Mechanical Engineering Education, Key Laboratory of High Efficiency and Clean Mechanical Manufacture of MQE, Jinan 250061, China

\* Correspondence: melius@sdu.edu.cn; Tel./Fax: +86-531-8839-3206

**Abstract:** Engineering components are usually manufactured with sequential production processes. Work hardening due to previous production processes affects the machinability of the workpiece in subsequent operations. In this research, the surface work hardening of a workpiece manufactured by two sequential processes with heat treatment/milling (HT + M) and milling/heat treatment (M + HT) of superalloy GH4169 was investigated. First, the surface microstructure characteristics, including plastic deformation and grain size of the machined workpiece surface processed by the two sequential processes, were quantitatively presented. Then, the microhardness on the machined workpiece surface and its cross-section was measured and analyzed. Finally, a surface microhardness calculation model considering twin boundary deformation was proposed. Here, we also present the microstructure evolution principle of the machined workpiece surface by the two sequential processes. It was found that the degree of work hardening of HT + M machining was 179%, whereas that of M + HT was only 101%. The research results can be applied to the optimized selection of process sequence for manufacturing superalloy GH4169.

**Keywords:** milling; solution heat treatment; work hardening; sequential production processes



**Citation:** Zhu, P.; Liu, Z.; Ren, X.; Wang, B.; Song, Q. Effects of Sequential Operation with Heat Treatment and Mechanical Milling on Work Hardening for Superalloy GH4169. *Metals* **2021**, *11*, 1367. <https://doi.org/10.3390/met11091367>

Academic Editors: Matjaž Godec and Danijela Skobir Balantić

Received: 28 July 2021

Accepted: 27 August 2021

Published: 30 August 2021

**Publisher's Note:** MDPI stays neutral with regard to jurisdictional claims in published maps and institutional affiliations.



**Copyright:** © 2021 by the authors. Licensee MDPI, Basel, Switzerland. This article is an open access article distributed under the terms and conditions of the Creative Commons Attribution (CC BY) license (<https://creativecommons.org/licenses/by/4.0/>).

## 1. Introduction

Nickel-based superalloy GH4169 (Inconel 718) can maintain good comprehensive performance at a high temperature and is widely used in hot-end components, such as turbine discs and the turbine blades of an aero-engine [1]. However, the excellent high temperature strength leads to poor machinability of GH4169 alloy, which is mainly manifested in a significant tendency toward work hardening [2]. A large degree of work hardening can improve the microhardness and strength of the workpiece surface, but increases the difficulty of subsequent cutting operations and affects the surface quality of the finished machined parts [3].

Surface microhardness is an index used to evaluate the mechanical properties of workpieces. It is closely related to the microstructure of materials. The mechanical and thermal loads exerted by the machining process cause severe plastic deformation on the workpiece surface, which leads to changes in the microstructure of the material, including grain refinement and phase transformation, and, accordingly, changes in the microhardness of the machined surface [4]. Several researchers have studied the effect of cutting parameters on work hardening through microstructure change and obtained the optimal cutting parameters [5,6]. However, the production of superalloy GH4169 workpieces requires multiple production processes, such as heat treatment and cutting operations. Thus, consideration should not be limited to only the influence of a single cutting process on the workpiece surface quality.

The effects of heat treatment and the cutting process on the workpiece surface quality have been previously studied. As a post-treatment process, heat treatment can change the microstructure of the machined surface of a metal material by recrystallization in the hardened area. Yadav et al. [7] investigated the effect of heat treatment on the microstructure and mechanical properties of Inconel 718 chips formed in the cutting process. The workpiece was machined and then heat treated at different temperatures. It was found that recrystallization occurred on the machined surface in the plastic deformation zone, and that the extent of recrystallization could be controlled by heat treatment to improve the thermal stability and microhardness. The effects of grinding and annealing on the microstructure and mechanical properties were analyzed by Sina et al. [8]. They found that work hardening caused by machining can be reduced by heat treatment by means of recrystallization. In the studies of Yadav and Sina, their process procedure (machining followed by heat treatment) was not able to completely eliminate work hardening. The study of Wang Y. et al. [9] also found that further heat treatment is necessary to improve the microstructure of Inconel 718, because recovery and recrystallization occur. Heat treatment can change the content and distribution of the strengthening phase in the superalloy GH4169, which determines the material properties, and further affects the subsequent machinability of the material. Careri et al. [10] studied the effects of heat treatment and the cutting process on the surface integrity of nickel-based superalloys. These results showed that the material without strengthening by heat treatment achieved better machinability; however, the work hardening was greater and was not accurately predicted. Neslusan et al. [11] addressed the influence of heat treatment on machining process. The regime of heat treatment significantly affects aspects of the material such as structure and hardness, which can influence the final results in terms of cycle times and surface integrity. Hongliang et al. [12] studied the work hardening characteristics of a nickel-based superalloy at different temperatures of solution heat treatment. The solution treatment was optimized through the dissolving temperature of precipitations and the mean size of grains. The strain hardening exponent of the nickel-based superalloy first increased and then decreased during cold deformation. Several other papers have shown that heat treatment can affect the work hardening behavior of the machining workpiece by changing the microstructure of nickel-based alloys [1,13,14].

The objective of this study was to examine the microhardness distribution on the workpiece surface of GH4169 processed by sequential operations of solution heat treatment and a milling operation, and to reveal the work hardening mechanism required to optimize the selection of the process sequence for GH4169 production operations. The microstructural deformation features of the processing workpiece surface were characterized using a scanning electron microscope (SEM) and a laser confocal microscope. Based on the results of the experiment, a surface microhardness calculation model was proposed to understand the work hardening of GH4169.

## 2. Materials and Methods

### 2.1. Materials

The nickel-based superalloy GH4169 was used to study the effect of the sequential processes of heat treatment and milling on the microstructural evolution and microhardness of the machined surface. The as-received GH4169 was preheated during manufacture with process parameters of  $960 \pm 10$  °C, 4 h, water cooling,  $720 \pm 10$  °C, 9 h, furnace cooling at  $55$  °C/h to  $620 \pm 10$  °C, 8 h, air cooling. The chemical composition of the as-received GH4169 is shown in Table 1.

**Table 1.** Chemical composition of as-received GH4169 (wt.%).

Element	Ni	Cr	Fe	Nb	Mo	Ti	Al	Mn	Si	C	Co
Component	52.6	19.2	16.4	5.1	3.0	1.0	0.51	0.02	0.1	0.04	0.1

The initial microstructure of the material is shown in Figure 1. As shown in Figure 1a, the microstructure of GH4169 comprises equiaxed grains and a large number of straight twin boundaries. The average grain size is about 95  $\mu\text{m}$ , and the matrix microhardness is  $443 \pm 10$  HV. Two types of strengthening precipitates exist in GH4169, namely  $\gamma''$  ( $\text{Ni}_3\text{Nb}$ ) and  $\gamma'$  ( $\text{Ni}_3(\text{Al}, \text{Ti})$ ) [15], as shown in Figure 1b.

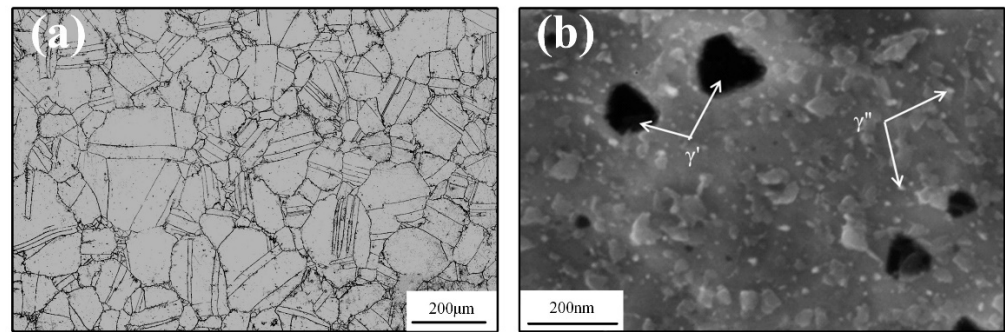


**Figure 1.** Initial microstructure of superalloy GH4169: (a) the grain microstructure; (b) the  $\gamma''$  and  $\gamma'$  phases.

## 2.2. Experimental Procedure

The effects of sequential processes of milling (down-milling) and solution heat treatment on work hardening were experimentally studied. Two sequential processes of manufacturing GH4169 were designed. In the process of M + HT, the workpiece was machined with a milling operation, then handled by solution heat treatment. The workpiece was manufactured with solution heat treatment and a subsequent milling operation in another process of HT + M. The sequential processes of manufacturing GH4169 and the nomenclature are shown in Figure 2 and Table 2, respectively.

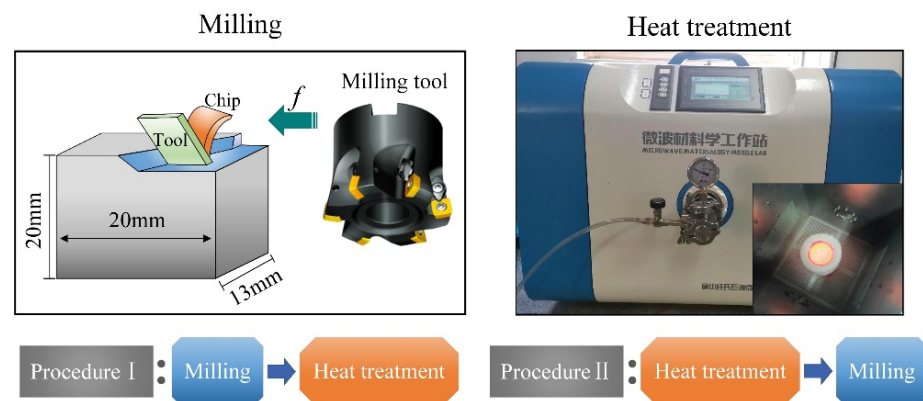


**Figure 2.** Sequential processes of manufacturing the GH4169 workpiece.

**Table 2.** Sample nomenclature.

Sample Condition	Sample Nomenclature
Milling	M
Heat treatment	HT
Milling and heat treatment at 960 °C for 1 h	M + HT
Heat treatment at 960 °C for 1 h and milling	HT + M

A face milling cutter head, model XMR01-063-A27-SD09-06, was used in the experiment. A carbide cutting tool with a rake angle of  $0^\circ$  and a clearance angle of  $15^\circ$  was used to machine the workpiece. The cutting parameters were set as follows: the cutting speed was 120 m/min, the feed rate of each tooth was 0.2 mm/z, the axial cutting depth was

0.2 mm, and the cutting width was 13 mm. The solution heat treatment was undertaken using a muffle furnace. The heat treatment process parameters were  $960 \pm 10$  °C, 1 h, air cooling.

After the experiment, sections of the workpieces manufactured by the two sequential processes were cut from the cross-section perpendicular to the feed direction using wire electrical discharge machining (WEDM). Then, sections were ground and polished to a mirror surface without scratches. Microhardness measurements were obtained by Vickers micro-indentation hardness testing method with a diamond indenter subjected to a load of 50 g. Finally, the microstructure of GH4169 after sequential processes was examined using a scanning electron microscope (SEM) and a laser confocal microscope (LCM). For SEM and LCM examinations, samples after mechanical polishing (with Sic to a grit size of 2000) were chemically etched. The chemical etchant comprised 0.5 g  $\text{CuCl}_2$ , 10 ml HCl, and 10 ml ethanol, and the etching time was 40 s.

### 3. Results and Discussion

#### 3.1. Microstructure Analysis of Sequential Machined GH4169 Surface

Figure 3 shows the evolution procedure of the surface microstructure generated in the sequential production processes. The initial microstructure of GH4169 is shown in Figure 3a. After the workpiece was machined, the machined surface produced a certain degree of plastic deformation, which was mainly characterized by the bending deformation of twin boundaries that were straight lines before machining (Figure 3b). When the machined workpiece was heat treated, the surface microstructure generated during machining was completely changed. The deformed grains caused by the cutting operation disappeared, and fine equiaxed grains were formed by recrystallization (Figure 3c). However, when the as-received GH4169 was processed by the HT + M process, different changes appeared on the workpiece surface in the microstructure compared with the M + HT workpiece. All grains grew significantly after the material was heat treated (Figure 3d). The severe plastic deformation occurred on the workpiece surface during the machining process after the as-received GH4169 was heat treated (Figure 3e). Compared with the surface of the M workpiece (Figure 3b), more grains of the HT + M workpiece surface were elongated in the horizontal direction and more twin boundaries were bent.

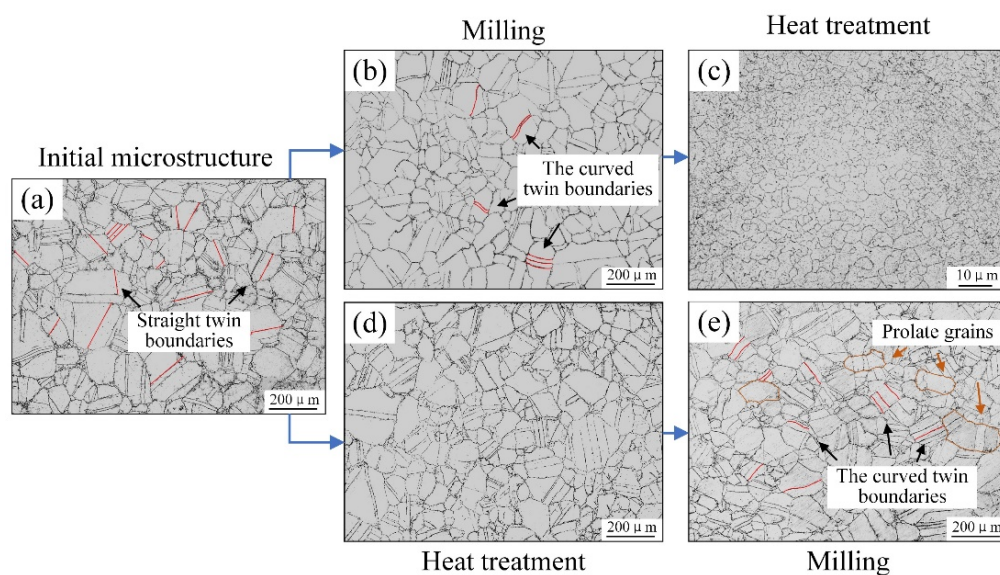


**Figure 3.** Surface microstructure generated in sequential production process: (a) initial microstructure of workpiece surface; (b) machined surface; (c) heat treated surface after machining; (d) heat treated surface of the as-received material; (e) machined surface after heat treatment.

Surfaces with a different microstructure were obtained by the two sequential production processes. In the M + HT process, a small degree of plastic deformation (a small number of curved twin boundaries) occurred on the workpiece surface followed by recrystallization. Finally, a surface without plastic deformation with fine grains was obtained. In contrast, in the HT + M process, grains grew first, then a large degree of plastic deformation (more curved twin boundaries and prolate grains) occurred on the machined surface. Finally, a plastic deformed surface with large grains was obtained.

The microstructures of the cross-section near the machined surface processed in the sequential production processes are shown in Figure 4a–c. As shown in Figure 4a,b, the red curves represent the position of the twin boundary before and after the machining process. After the as-received GH4169 was machined, the bending deformation degree of the twin boundary was small, characterized by the position of the solid line and the dotted line, and the deformation depth was about 15  $\mu\text{m}$ . By comparison, the deformation depth of the twin boundary was about 40  $\mu\text{m}$  for the workpiece processed by the HT + M process. The deformation degree of the HT + M workpiece was much larger than that of the M workpiece. Figure 4c shows the microstructure of the cross-section of the workpiece processed by the M + HT process. The red curves in Figure 4c represent the grain boundaries of the recrystallized grain. It can be seen from Figure 4c that the recrystallized grain near the machined surface was the smallest and the depth of the recrystallized area was about 30  $\mu\text{m}$ .

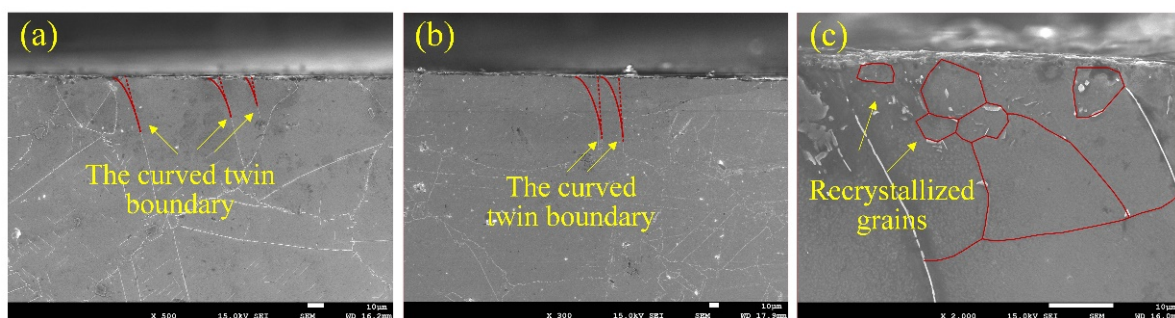


**Figure 4.** Microstructure of the GH4169 workpiece cross-section: (a) milling workpiece; (b) HT + M workpiece; (c) M + HT workpiece.

### 3.2. Grain Size of Sequential Machined GH4169 Surface

From the microstructural analysis, it is evident that the machining and heat treatment process can cause changes in the grain size. Because mechanical properties, particularly strength and microhardness, are directly dependent upon the grain size, the laser confocal microscope was used to measure the average grain size of the surface under various process conditions. The measurement results are shown in Figure 5. It is clear that there was a moderate decrement in grain size after the workpiece was machined and a drastic decrement in grain size after the machined workpiece was heat treated. The average grain size of the as-received GH4169 was 95  $\mu\text{m}$ . After the workpiece was machined at the cutting speed of 120 m/min, the surface grain size decreased by 18% (M process), whereas the average grain size was 3  $\mu\text{m}$  after the machined workpiece was heat treated at 960  $^{\circ}\text{C}$  for one hour (M + HT process). In the HT + M process, the average grain size increased from 95 to 110  $\mu\text{m}$  when the as-received GH4169 was heat treated. After the heat-treated workpiece was machined, the surface grain size decreased by 24%. The grain refinement degree of the machined surface in the HT + M process was larger than that of the M process.

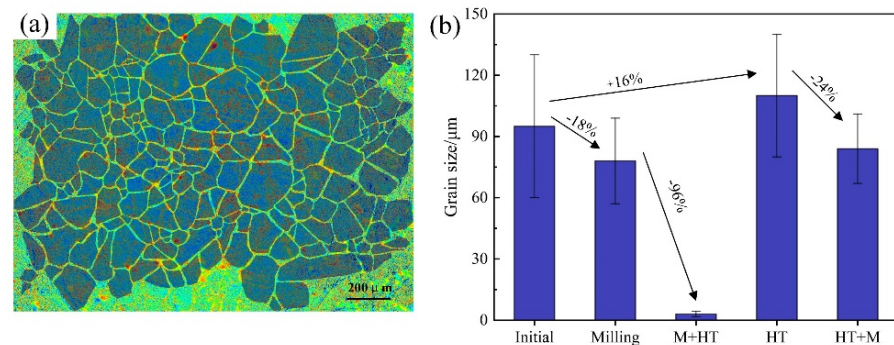


**Figure 5.** The surface grain size generated in the sequential production process: (a) the processed surface; (b) the grain size.

### 3.3. Surface and Sub-Surface Microhardness of Sequential Machined GH4169

It was found that the surface microstructure of the workpiece underwent changes after the M + HT and HT + M processes were performed on the as-received GH4169. The microhardness of GH4169 is closely related to its microstructure [16]. After the sequential production processes, the surface microhardness was measured for various workpiece conditions, as shown in Figure 6. The bar chart shows the microhardness of the workpiece matrix and the surface (HV<sub>0</sub>, HV), and the line chart shows the degree of work hardening (HV/HV<sub>0</sub> × 100%). It is clear from Figure 6 that there was a significant decrement in the matrix hardness from the as-received GH4169 (443 ± 10 HV<sub>0.05</sub>) to the heat-treated state (240 ± 5 HV<sub>0.05</sub>). Thus, it can be concluded that the solution heat treatment made the material soft. Previous studies have shown that heat treatment above 750 °C induced dissolution of γ'' and γ' nanoprecipitates, which should lead to the strengthening of GH4169 [17,18].

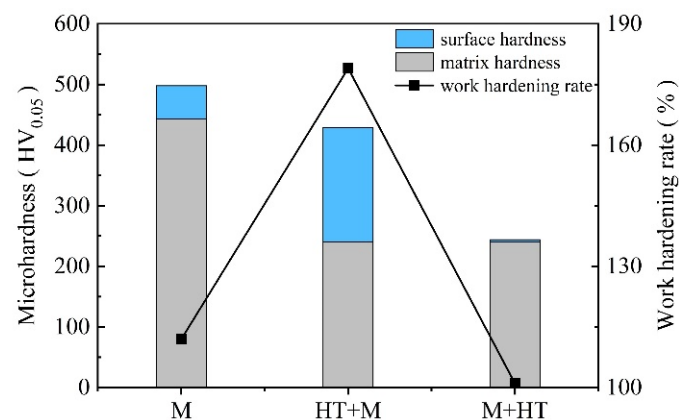


**Figure 6.** Surface microhardness and degree of work hardening of sequential machined workpieces.

Comparing the microhardness on the surface of GH4169 processed by the sequential production processes, it can be found that the surface microhardness of the M workpiece was the largest (498 ± 10 HV). The value of the microhardness of the HT + M workpiece surface was ranked second (429 ± 10 HV), and the result of the M + HT workpiece was the smallest (244 ± 5 HV). However, the degree of work hardening of the workpiece processed by the HT + M process was the highest, followed by that of the M process, and that of the workpiece processed by M + HT process was the lowest. Their values were 179%, 112%, and 101%, respectively. According to the results, it should be noted that, although the degree of work hardening of the HT + M workpiece was very high, the microhardness on surface was still less than that of the as-received material. Furthermore, the work hardening of the M + HT workpiece was only 101%; that is, no work hardening occurred on the surface of the workpiece that underwent the M + HT process.

Due to the mechanical load caused by the application of the tool to the workpiece during the cutting operation, not only was the workpiece surface strengthened, but the subsurface microhardness of the workpiece was also changed. Microhardness measurements were tested in cross-section from the machined surface for M, HT + M, and M + HT processes. The microhardness profiles for the three workpiece conditions, beginning from the machined surface and ending 120  $\mu\text{m}$  into the workpiece, are shown in Figure 7. It can be seen from Figure 7 that the microhardness of the cross-section presented a gradient distribution along the depth direction. The microhardness on the surface reached the highest value and then decreased to the value of the matrix area. The HT + M workpiece showed the largest variation of microhardness, followed by the M workpiece. The M + HT workpiece had the smallest variation. Their work hardening depths were 75, 45, and 0  $\mu\text{m}$ , respectively. The HT + M process resulted in a significant hardening gradient and depth on the processed surface of the workpiece, whereas the surface microhardness of the workpiece processed by the M + HT process was the same as that of the matrix; that is, the work hardening caused by the cutting operation was eliminated by the solution heat treatment.

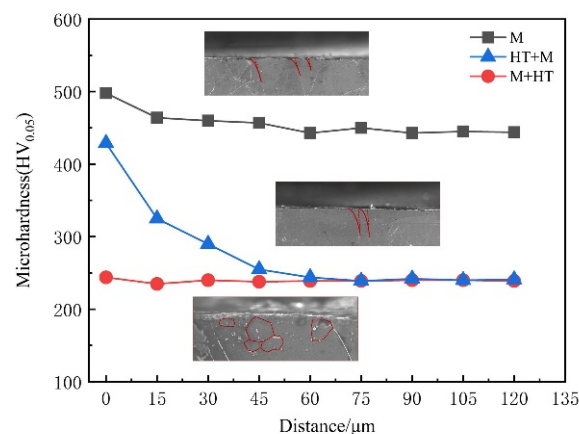


**Figure 7.** Microhardness distribution of the cross-section for M, HT + M, and M + HT conditions.

### 3.4. Relationship between Microstructure and Work Hardening

Plastic deformation in the cutting process of superalloy GH4169 is commonly accommodated by twinning and slip. The deformation twin is mainly formed during the high-speed cutting operation, whereas the plastic deformation in the low-speed cutting operation is accommodated by slip [19]. During the machining process, dislocations caused by plastic strain produce the dislocation pile-up at the grain boundary and the twin boundary. The dislocation pile-up has a repulsive force on subsequent dislocations, which is proportional to the number of dislocations in the dislocation pile-up group [20]. When dislocations of the dislocation pile-up reach a certain number ( $n$ ), the external force cannot induce new plastic deformation, which produces dislocations; thus, work hardening occurs on the machined surface. The relationship between the number of dislocations in the dislocation pile-up and shear stress is shown in Equation (1):

$$N \approx K\pi\tau_0L/Gb \quad (1)$$

where  $K$  is the coefficient related to the dislocation type,  $\tau_0$  is the applied effective shear stress driving the dislocation movement, and  $L$  is the length of the dislocation pile-up group, namely the distance between the dislocation source and the grain boundary. According to Equation (1), a small length of the dislocation pile-up group ( $L$ ) means a small number of dislocations when the effective shear stress  $\tau_0$  is constant.

The Hall–Petch equation is a microhardness calculation model based on grain size, as expressed by Equation (2) [21]:

$$HV = HV_0 + kd^{-1/2} \quad (2)$$

where  $HV$  is the microhardness of the material,  $HV_0$  is the initial microhardness,  $d$  is the average grain size of the material, and  $k$  is the coefficient. Smaller grains have more grain boundaries, which can hinder dislocation slip. During the cutting process, the dislocation movement needs to overcome the increase in resistance due to the accumulation of dislocations at the grain boundary. Therefore, a metal material with a smaller grain size has higher strength and microhardness.

The superalloy GH4169 used in this study contains a large number of twin boundaries. The Hall–Petch equation for predicting material microhardness based on grain size only considers the effect of grain boundaries on dislocation slip, and does not consider the effect of a large number of twin boundaries. It can be seen from the microstructure of the machined surface (Figures 3 and 4) that twinning boundaries inside the grain were bent due to the plastic deformation during the machining process. This indicates that the twin boundary was resistant to shear deformation during the cutting operation and a large number of dislocations would form a dislocation pile-up at the twin boundary.

Therefore, a new microhardness calculation model considering twin boundary deformation was proposed to explain the work hardening for GH4169. The elastic moduli of the grain boundary, the twin boundary, and the grain of GH4169 are considered to be the same. There are two twin boundaries, on average, inside the grain. The thickness of the grain and twin boundaries is  $t$ . The yield stress of the material is  $\sigma_y$ , where  $\sigma_{fG}$  and  $\sigma_{fGB}$  are the yield stress within the grain and the yield stress at the grain boundary, respectively [22]:

$$\sigma_y = A_G\sigma_{fG} + A_{GB}\sigma_{fGB} \quad (3)$$

$$t = k_{MA}d_{avg}^{1/2} \quad (4)$$

$$A_G = \frac{\frac{1}{4}\pi(d_{avg} - 2t)^2 - 2t(d_{avg} - 2t)}{\frac{1}{4}\pi d_{avg}^2} \quad (5)$$

$$A_{GB} = \frac{\frac{1}{4}\pi(d_{avg}^2 - (d_{avg} - 2t)^2) - 2t(d_{avg} - 2t)}{\frac{1}{4}\pi d_{avg}^2} = 1 - A_G \quad (6)$$

where  $A_G$  is the proportion fraction of the area inside the grain to the total grain area,  $A_{GB}$  is the proportion fraction of the area of the grain boundary and the twin boundary to the total grain area,  $k_{MA}$  is the coefficient, and  $d_{avg}$  is the average grain diameter.  $A_G$  and  $A_{GB}$  are substituted into Equation (3) to obtain Equation (7):

$$\sigma_y = \sigma_{fG} + \frac{16 + 8\pi}{\pi}k_{MA}(\sigma_{fGB} - \sigma_{fG})d_{avg}^{-1/2} - \frac{64 + 16\pi}{\pi}k_{MA}^2(\sigma_{fGB} - \sigma_{fG})d_{avg}^{-1} \quad (7)$$

Tabor has given the relationship between the ultimate strength  $\sigma_u$  and the microhardness  $HV$ , as shown in Equation (8) [23]:

$$\sigma_u = \frac{HV}{2.9} \left( \frac{n}{0.217} \right)^n \quad (8)$$

where  $n$  is the strain hardening coefficient.

The relationship between the ultimate strength  $\sigma_u$  and the yield strength  $\sigma_y$  is expressed as Equation (9):

$$\sigma_u = C\sigma_y \quad (9)$$

where  $C$  is a coefficient, which was found to be equal to 0.801 [24].

Equations (8) and (9) are substituted into Equation (7) to obtain Equation (10). Then, a new microhardness calculation model is developed which facilitates the understanding of work hardening for the superalloy GH4169:

$$HV = \frac{2.9 \times 0.217^n}{0.801 \times n^n} \times [\sigma_{fG} + \frac{16 + 8\pi}{\pi} k_{MA} (\sigma_{fGB} - \sigma_{fG}) d_{avg}^{-1/2} - \frac{64 + 16\pi}{\pi} k_{MA}^2 (\sigma_{fGB} - \sigma_{fG}) d_{avg}^{-1}] \quad (10)$$

The microhardness of the as-received GH4169 was very high and decreased by 46% after the solution heat treatment was performed. Compared with low hardness, this high degree of hardness would result in slight plastic deformation on the workpiece surface during the cutting operation. As can be seen from the microstructure of the cross-section in Figure 4, the plastic deformation depth of the M and HT + M workpieces was 15 and 40  $\mu\text{m}$ , respectively. Due to the slight plastic deformation on the machined surface, a small number of dislocations accumulated at the grain boundary. As a result, the degree of work hardening and depth of work hardening of the M workpiece were only 112% and 45  $\mu\text{m}$ , respectively. Under the same machining parameters, the grain boundary of the HT + M workpiece was able to accumulate a mass of dislocations due to significant plastic deformation. Therefore, the degree of work hardening and depth of work hardening of the HT + M workpiece reached 179% and 70  $\mu\text{m}$ , respectively. The evolution procedure of the processed surface microstructure of the workpiece treated by the HT + M process is shown in Figure 8.

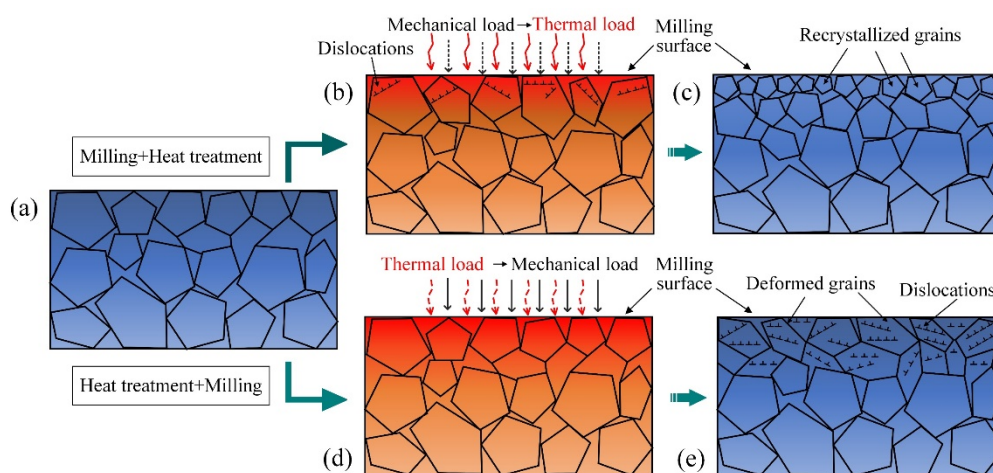


**Figure 8.** Schematic diagram of microstructure evolution of the machined workpiece surface by sequential production process: (a) original equiaxed grained microstructure; (b) a small number of dislocations formed within grains due to milling; (c) recrystallized grains without dislocations formed on the milling surface after the M + HT process; (d) original grains' growth due to heat treatment; (e) elongated grains with a large number of dislocations formed on the surface after the HT + M process.

In the machining process of GH4169, most of the work performed by the cutting force on the workpiece surface was lost through the chip in the form of heat. The remaining energy was stored on the machined surface in the form of increasing crystal defects, composed mainly of dislocations [25]. The machined surface was in an unstable high-energy state due to the increase in stored energy. When it was heat-treated, the stored energy acted as a driving force to promote recrystallization [26].

As can be seen from Figure 4c, the cross-section of the M + HT workpiece near the machined surface was composed of recrystallized grains, which showed a gradient structure. After the as-received GH4169 was machined, the dislocation density on the subsurface was in a gradient distribution, namely, the dislocation density gradually decreased from the machined surface to the matrix [27]. As a result, the driving force of recrystallization on the machined surface was larger than that on the subsurface during the heat treatment. Thus,

the recrystallization presented a gradient structure on the cross-section. According to the experimental results, the depth of work hardening of the M process and the recrystallization depth of the M + HT process were 45 and 30  $\mu\text{m}$ , respectively. Hence, it can be said that recrystallization occurred within the area of work hardening and the solution heat treatment can eliminate the work hardening caused by the machining process by means of recrystallization. The evolution procedure of the processed surface microstructure of the workpiece treated by the M + HT process is also shown in Figure 8. In addition, although the grains on the processed surface of the workpiece treated by the M + HT process were refined, the microhardness on this surface was similar to that of the matrix. The refined grains did not improve the microhardness of the surface because the strengthening phase was dissolved at the same time by the heat treatment. The material composition tended to be uniform after the heat treatment was performed, which resulted in the disappearance of the microhardness gradient on the machined surface [28].

#### 4. Conclusions

The effects of sequential production processes (HT + M and M + HT) on the work hardening of superalloy GH4169 were studied. Microstructure characterization and microhardness analysis offered relevant evidence for the choice of the manufacturing process in superalloy GH4169. A surface microhardness calculation model considering twin boundary deformation was proposed, and the evolution procedure of the workpiece surface microstructure in the sequential production processes was discussed. The main conclusions are summarized as follows.

- There was a degree of plastic deformation on the workpiece surface during the machining process, which was characterized by grain deformation and twin boundary bending. The degree and depth of plastic deformation of the workpiece surface processed by the HT + M process were greater than those of the M process. The plastic deformation depths beneath the machined surface under the two conditions were 15 and 40  $\mu\text{m}$ , respectively, whereas the machined surface was recrystallized with a depth of 30  $\mu\text{m}$  in the M + HT process.
- Grains on the surface subjected to the sequential production processes were refined to different degrees. The grain size of the as-received GH4169 was 95  $\mu\text{m}$  and grew to 110  $\mu\text{m}$  after the solution heat treatment was performed. The surface grain sizes of the workpiece were reduced to 78 and 84  $\mu\text{m}$  in M and HT + M processes, respectively. The recrystallized grain size of the workpiece surface processed by the M + HT process was 3  $\mu\text{m}$ .
- According to the grain refinement and twin boundary bending, a surface microhardness calculation model was proposed to explain the work hardening for GH4169.
- The effects of the M + HT and HT + M processes on the work hardening of the workpiece surface were significantly different. In the M + HT process, a surface with a low degree of work hardening (112%) and a small deformation depth (15  $\mu\text{m}$ ) was first formed. Then, a surface without work hardening was formed by recrystallization. In the HT + M process, grains grew first; then, a surface with a high degree of work hardening (179%) and a large deformation depth (40  $\mu\text{m}$ ) was formed.

**Author Contributions:** Conceptualization, Q.S.; methodology, Z.L.; validation, X.R.; investigation, P.Z.; resources, B.W.; writing—original draft preparation, P.Z.; writing—review and editing, Z.L., X.R. and B.W.; project administration, Z.L. All authors have read and agreed to the published version of the manuscript.

**Funding:** This research was funded by National Natural Science Foundation of China (No. 91862027) and National Key Research and Development Program of China (2019YFB2005401).

**Institutional Review Board Statement:** Not applicable.

**Informed Consent Statement:** Not applicable.

**Data Availability Statement:** The data presented in this study are available within the article.

**Conflicts of Interest:** The authors declare no conflict of interest. The funders had no role in the design of the study; in the collection, analyses, or interpretation of data; in the writing of the manuscript, or in the decision to publish the results.

## References

1. Detrouis, M.; Antonov, S.; Tin, S.; Jablonski, P.D.; Hawk, J.A. Hot deformation behavior and flow stress modeling of a Ni-based superalloy. *Mater. Charact.* **2019**, *157*, 109915. [CrossRef]
2. De Souza, G.R.; Gabriel, S.B.; Dille, J.; dos Santos, D.S.; de Almeida, L.H. Work hardening and aging contribution on the mechanical properties of X-750 nickel-based superalloy. *Mater. Sci. Eng. A* **2013**, *564*, 102–106. [CrossRef]
3. Çetinkaya, S.K.; Kacal, A.A. Investigation of the heat treatment effect in milling of K390 powder metallurgical steel. *Kov. Mater.-Met. Mater.* **2014**, *52*, 209–218. [CrossRef]
4. Liao, Z.; Polyakov, M.; Diaz, O.G.; Axinte, D.; Mohanty, G.; Maeder, X.; Hardy, M. Grain refinement mechanism of nickel-based superalloy by severe plastic deformation-Mechanical machining case. *Acta Mater.* **2019**, *180*, 2–14. [CrossRef]
5. Yin, Q.; Liu, Z.; Wang, B.; Song, Q.; Cai, Y. Recent progress of machinability and surface integrity for mechanical machining Inconel 718: A review. *Int. J. Adv. Manuf. Technol.* **2020**, *109*, 215–245. [CrossRef]
6. Zhang, S.; Li, W.; Guo, Y.B. Process design space for optimal surface integrity in finish hard milling of tool steel. *Prod. Eng.* **2012**, *6*, 355–365. [CrossRef]
7. Yadav, P.C.; Sahu, S.; Subramaniam, A.; Shekhar, S. Effect of heat-treatment on microstructural evolution and mechanical behaviour of severely deformed Inconel 718. *Mater. Sci. Eng. A* **2018**, *715*, 295–306. [CrossRef]
8. Shahrezaei, S.; Sun, Y.; Mathaudhu, S.N. Strength-ductility modulation via surface severe plastic deformation and annealing. *Mater. Sci. Eng. A* **2019**, *761*, 138023. [CrossRef]
9. Wang, Y.; Shi, J. Effect of post heat treatment on the microstructure and tensile properties of nano tic particulate reinforced inconel 718 by selective laser melting. *J. Manuf. Sci. Eng.* **2020**, *142*, 051004. [CrossRef]
10. Careri, F.; Imbrogno, S.; Umbrello, D.; Attallah, M.M.; Outeiro, J.; Batista, A.C. Machining and heat treatment as post-processing strategies for Ni-superalloys structures fabricated using direct energy deposition. *J. Manuf. Process.* **2021**, *61*, 236–244. [CrossRef]
11. Neslusan, M.; Mrkvica, I.; Cep, R.; Kozak, D.; Konderla, R. Deformations after heat treatment and their influence on cutting process. *Tech. Gaz.* **2011**, *4*, 601–608. Available online: <http://hrcak.srce.hr/file/111986> (accessed on 27 August 2021).
12. Hongliang, L.; Maicang, Z.; Min, X.; Ye, M.; Guohua, X.; Na, T.; Lei, Z. Microstructure evolution dependence of work-hardening characteristic in cold deformation of a difficult-to-deform nickel-based superalloy. *Mater. Sci. Eng. A* **2021**, *800*, 14028. [CrossRef]
13. Semiatin, S.L.; McClary, K.E.; Rollett, A.D.; Roberts, C.G.; Payton, E.J.; Zhang, F.; Gabb, T.P. Plastic flow and microstructure evolution during thermomechanical processing of a PM Nickel-Base superalloy. *Metall. Mater. Trans. A* **2013**, *44*, 2778–2798. [CrossRef]
14. Zhongnan, B.; Maicang, Z.; Jianxin, D.; Kunjie, L.; Jue, W. A new prediction model of steady state stress based on the influence of the chemical composition for nickel-base superalloys. *Mater. Sci. Eng. A* **2010**, *527*, 4373–4382. [CrossRef]
15. Ren, X.P.; Liu, Z.Q. Microstructure refinement and work hardening in a machined surface layer induced by turning Inconel 718 super alloy. *Int. J. Miner. Metall. Mater.* **2018**, *25*, 937–949. [CrossRef]
16. Zhao, Y.; Guo, Q.; Ma, Z.; Yu, L. Comparative study on the microstructure evolution of selective laser melted and wrought IN718 superalloy during subsequent heat treatment process and its effect on mechanical properties. *Mater. Sci. Eng. A* **2020**, *791*, 139735. [CrossRef]
17. Sohrabi, M.J.; Mirzadeh, H. Unexpected formation of delta ( $\delta$ ) phase in as-cast niobium-bearing superalloy at solution annealing temperatures. *Mater. Lett.* **2020**, *261*, 127008. [CrossRef]
18. An, X.L.; Zhang, B.; Chu, C.L.; Zhou, L.; Chu, P.K. Evolution of microstructures and properties of the GH4169 superalloy during short-term and high-temperature processing. *Mater. Sci. Eng. A* **2019**, *744*, 255–266. [CrossRef]
19. Wang, Q.; Liu, Z. Plastic deformation induced nano-scale twins in Ti-6Al-4V machined surface with high speed machining. *Mater. Sci. Eng. A* **2016**, *675*, 271–279. [CrossRef]
20. Blum, W.; Zeng, X.H. A simple dislocation model of deformation resistance of ultrafine-grained materials explaining Hall–Petch strengthening and enhanced strain rate sensitivity. *Acta Mater.* **2009**, *57*, 1966–1974. [CrossRef]
21. Shaw, L.L.; Ortiz, A.L.; Villegas, J.C. Hall–Petch relationship in a nanotwinned nickel alloy. *Scr. Mater.* **2008**, *58*, 951–954. [CrossRef]
22. Meyers, M.A.; Ashworth, E. A model for the effect of grain size on the yield stress of metals. *Philos. Mag. A* **1982**, *46*, 737–759. [CrossRef]
23. Cahoon, J.R. An improved equation relating hardness to ultimate strength. *Metall. Mater. Trans. B* **1972**, *3*, 3040. [CrossRef]
24. Ren, X.; Liu, Z. Influence of cutting parameters on work hardening behavior of surface layer during turning superalloy Inconel 718. *Int. J. Adv. Manuf. Technol.* **2016**, *86*, 2319–2327. [CrossRef]
25. Fan, Y.; Wang, W.; Hao, Z.; Zhan, C. Work hardening mechanism based on molecular dynamics simulation in cutting Ni–Fe–Cr series of Ni-based alloy. *J. Alloys Compd.* **2020**, *819*, 153331. [CrossRef]
26. Chen, Z.; Moverare, J.J.; Peng, R.L.; Johansson, S.; Gustafsson, D. On the conjoint influence of broaching and heat treatment on bending fatigue behavior of Inconel 718. *Mater. Sci. Eng. A* **2016**, *671*, 158–169. [CrossRef]

- 
27. Li, B.; Zhang, S.; Hu, R.; Zhang, X. Dislocation density and grain size evolution in hard machining of H13 steel: Numerical and experimental investigation. *J. Mater. Res. Technol.* **2020**, *9*, 4241–4254. [[CrossRef](#)]
  28. Gupta, C.; Jha, J.S.; Jayabalan, B.; Gujrati, R.; Alankar, A.; Mishra, S. Correlating hot deformation parameters with microstructure evolution during thermomechanical processing of inconel 718 alloy. *Metall. Mater. Trans. A* **2019**, *50*, 4714–4731. [[CrossRef](#)]